

# Synthesis and investigation of optical properties of CdSe quantum dots with high quantum luminescence yield

A.Z. Kainarbay<sup>\*1</sup>, T.N. Nurakhmetov<sup>1</sup>, Z.M. Salikhodja<sup>1</sup>,  
A.M. Zhunusbekov<sup>1</sup>, D.K. Daurenbekov<sup>1</sup>, B. Sadykova<sup>1</sup>,  
B. Yussupbekova<sup>1</sup>, K. Zhanylysov<sup>1</sup>, A. Kainarbayeva<sup>2</sup>,  
N. Adalbek<sup>2</sup>, N. Shaken<sup>1</sup>, A. Turmakhanbetova<sup>1</sup>,  
K.N. Balabekov<sup>1</sup>

<sup>1</sup>L.N. Gumilyov Eurasian National University, Astana, Kazakhstan

<sup>2</sup>Abai Kazakh State Pedagogical University, Almaty, Kazakhstan

E-mail: kainarbay\_azh@enu.kz

DOI: 10.29317/ejpfm.2018020405

Received: 20.11.2018 - after revision

In the present work, an attempt to obtain quantum dots with a high quantum luminescence yield has been made. For this purpose, the existing methods of synthesis have been studied; approbation of availability and reproducibility of the results and possibility of obtaining luminescent QD samples in the required spectral region has been made. The optical characteristics, the influence of the synthesis conditions, the possibility of using nanostructured materials for sensitization of solar cells have been studied.

**Keywords:** colloidal quantum dots, CdSe, synthesis, luminescence.

## Introduction

Interest to the synthesis and study of semiconductor nanoparticles, the so-called quantum dots (QDs) is caused by the study of their energy spectra and promising

practical applications [1]. The quantum-size effects played key role in the QD optical properties, which make possible to control the optical absorption or luminescence band by varying linear dimensions of nanoparticles. Depending on the method of synthesis, luminescent nanoparticles can be obtained with specified spectral characteristics. This becomes possible with a controlled change in the conditions of synthesis, for example, temperature and time, selection of chemical reagents, freezing conditions for the resulting nanoparticles, and other parameters. The dependence of the energy spectrum of semiconductor nanocrystalson from their size gives a high potential for their practical application [2].

Although studies of the luminescent properties of CdSe QDs have been carried out for a long time, and each research group has contributed to a better understanding of some physical quantities affecting the quantum yield (QY) of photoluminescence, many questions have not been answered yet. For example, the influence of the surface on the luminescent properties of QDs was disclosed in [3], but the relationship between surface quality, structural perfection, and nanoparticle growth has not yet been determined.

In [4], a simultaneous action of several parameters, such as synthesis temperature and time, and the influence of precursors on the luminescence quantum yield of CdSe QDs, was studied.

In many modern works on the synthesis of CdSe QDs, to increase QY, a mixture of coordinating solvents such as HDA (hexadecylamine), TOPO (tri-n-octylphosphine oxide), TOP (tri-n-octylphosphine) is used. It is worth noting that the luminescence quantum yield for CdSe QDs varies from (0.1-1.5)%. This composition of stabilizers also contributes to the establishment of an acceptable growth rate of nanoparticles and minimization of Oswald maturation. In [5, 6, 7] it was shown that this composition of stabilizers allows scientists to achieve a high QY value.

In this paper, an attempt has been made to systematize the existing methods, to test them, to study the effect of synthesis conditions, their variations on the physical properties of QDs, to study the effect of temperature, time and different ratio of stabilizers on QY and monodispersity of the nanoparticle ensemble.

*Synthesis.* In general, colloidal CdSe quantum dots were obtained by high-temperature organometallic synthesis, modification of existing techniques. This synthesis method is also called the molecular precursor method, in which precursors are separately prepared, for example cadmium oleate (precursor 1) and trioctylphosphine selenide (TOPSe, precursor 2). Further, the samples of the obtained nanoparticles will be denoted by their numbers. The main changes in the methods concerned selection of reagents, reaction volume, temperature and ratio of cadmium and selenium precursors.

A series of QD samples designated as No. 1 was obtained using a modified technique described in [8]; a series of samples obtained by the method given in [4, 6, 7] is designated as No. 2. For all QD samples, the ratio of Cd:Se precursors was 1:5 for a number of objective reasons [4].

*Synthesis #1* have been prepared according to [8] using a scaled up and modified procedure. Cadmium oleate was prepared by adding 0.133 g  $(\text{CH}_3\text{-COO})_2\text{Cd}\cdot 2\text{H}_2\text{O}$  to 0.6 ml oleic acid dissolved in 5 ml of diphenyl ether. The

solution was degassed, heated at 145 ° C under argon atmosphere and then heated to 240 ° C. TOP Se solution was obtained by dissolving 0.121 g of Se in 1.5 ml TOP. CdSe QD were prepared by injection TOP Se in Cd oleate in 3 - neck round bottom flask.

*Synthesis #2* have been prepared according to [4, 6, 7] using a scaled up and modified procedure. Cadmium oleate was prepared by adding 0.133 g (0.5 mmol)  $(\text{CH}_3\text{COO})_2\text{Cd}\cdot 2\text{H}_2\text{O}$  to 0.56 ml (2 mmol) oleic acid dissolved in 5 ml of diphenyl ether. The solution was degassed, heated to 145 ° C under argon atmosphere. and then heated to 240 ° C. TOP Se solution was obtained by dissolving 0.197 g (2.5 mmol) of Se in 1.5 ml TOP. CdSe QD were prepared by injection TOP Se in Cd oleate in 3 - neck round bottom flask. However, before this injection, a separately prepared mixture containing 1.34 g TOPO (63%) and 0.66 grams. HDA (33%) was added to the flask containing cadmium oleate. A mixture of TOPO:HDA is dried and degassed at 180 ° C at low vacuum, after heated in an atmosphere of argon. The ratio of the TOPO:HDA blend components changed as 63:33, 50:50, 33:63. However, the number of TOP remained unchanged in all cases.

As it is known, a CdSe nanocrystal can exist in two crystalline modifications: hexagonal and cubic. The presence of one or another structure depends on the type of selenium precursor [9, 10], for example, the use of selenium in the form of TOP Se (formation of trioctylphosphine selenide in TOP) leads to the formation of a hexagonal crystal lattice; selenium in 1-octadecene leads to the formation of a cubic structure. Thus, using uniform synthesis conditions, but different selenium precursors, one can obtain QDs of a different structure. A series of samples, obtained by the method given in [9], is designated as No. 3. We set the goal of determining the influence of the structural modification of QD on its optical-luminescent properties, which is why synthesis No. 3 is required.

*Synthesis #3.* A 0.1 M cadmium oleate precursor in ODE was prepared by adding 2 mmol of  $(\text{CH}_3\text{COO})_2\text{Cd}\cdot 2\text{H}_2\text{O}$  to 5 ml of oleic acid dissolved in 15 ml ODE. Subsequently the solution was degassed under reduced pressure, heated at 145 ° C for 45 minutes in an inert atmosphere (argon, 99.995%) until a clear solution was obtained. Then the temperature of the flask was raised to 240 ° C. To prepare the selenium precursor, 0.1975 g (2.5 mmol) of Se was dispersed in 1 ml ODE until completely dissolved.

To form CdSe QDs (sphalerite modifications), Se-ODE was injected into a flask containing cadmium oleate. For the formation of QD modification of wurtzite TOP Se was injected (0.1975 g of Se in 0.5 ml TOP).

*QD characterization.* All optical measurements were performed within 12 hours after the end of the synthesis. Optical absorption spectra were obtained on a JascoV770 spectrophotometer. Measurements were made in quartz cuvettes. The energy of the exciton transition obtained from the maximum of the first exciton absorption peak was used to estimate the average diameter of nanocrystals using the empirical formula given in [11]. The luminescence quantum yield was determined by comparison with the standard with a known quantum yield (Rhodamine 6G in ethanol) according to the procedure given in [12, 13]. The photoluminescence measurements were performed on a CM2203 spectrofluorometer at room temperature. The luminescence spectra are recorded at 90 ° C from the excitation beam.

For all QD samples, a small volume aliquot ( $\approx 0.1$  ml) is taken at regular intervals after injection of selenium precursor. Post-treatment purification procedures were not used to study the optical characteristics of the aliquots. When the last sample was taken, the reaction mixture was removed from the heat with rapid cooling to room temperature. The obtained colloidal QD solution was coagulated by addition of acetone, purified by washing with acetone and centrifugation (15 min., 8000 rpm). The resulting precipitate was redispersed in toluene, chloroform for long-term storage.

The XRD analysis was made on a D8 ADVANCE ECO diffractometer (Bruker, Germany) using  $\text{CuK}\alpha$  radiation. To identify the phases and to study the crystal structure, the software Bruker AXSDIFFRAC.EVA v.4.2 and the ICDD PDF-2 international database were used. Figure 1 shows X-ray diffraction patterns of the studied samples. The samples obtained are polycrystalline structures with strongly broadened asymmetric diffraction peaks. The asymmetric broadened form of diffraction peaks indicates the presence of a large number of lattice deformations in the structure. The Rietveld method was used to determine the phase state in the structure.

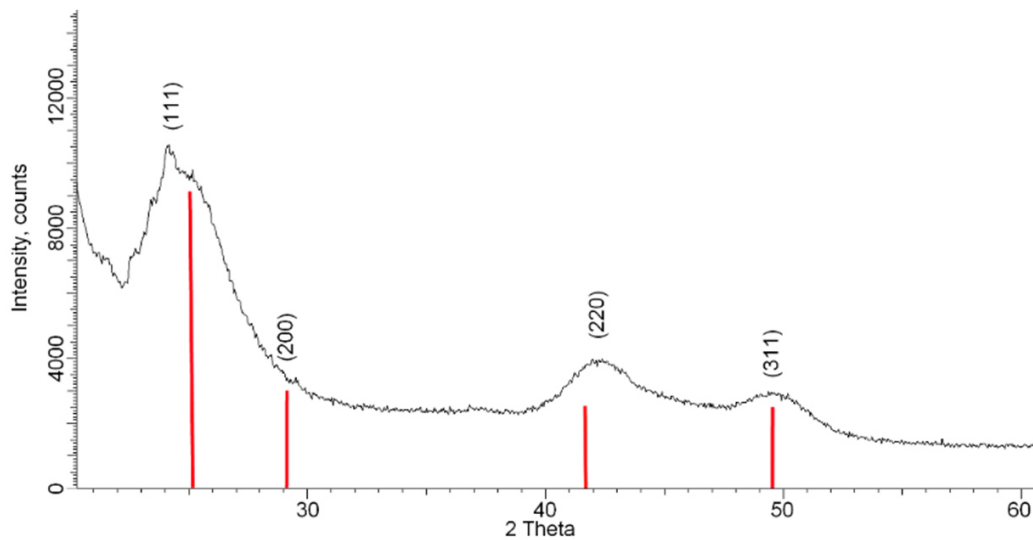


Figure 1. X-ray diffractogram of CdSe QDs, series No. 2, synthesis for 25 minutes at 240 ° C, the ratio of stabilizers TOPO:HDA = 50:50.

The contributions of deformation (defects of the first type) and changes in the size of crystallites (defects of the second type) were estimated using the Williamson-Hall method.

$$\beta^2 = \left( \frac{\lambda}{D \cdot \cos(\theta)} \right)^2 + (4 \cdot \varepsilon \cdot \tan(\theta))^2, \quad (1)$$

where  $\beta$  is the physical broadening of the diffraction maximum,  $\lambda$  is the X-ray wavelength (1.54 Å),  $D$  is the crystallite size,  $\theta$  is the Bragg diffraction angle,  $\varepsilon$  is the magnitude of micro stresses in the lattice. According to the estimation of the contributions, broadening of the diffraction peaks is caused both by a change in the sizes of crystallites and a change in the concentration of macro stresses in the structure. The lattice parameter was calculated using the Nelson-Taylor

extrapolation function. Table 1 presents the data on the phase composition and the main crystallographic characteristics.

Table 1.

Phase composition and the main crystallographic characteristics.

No.	Phase	Structure type	Spatial group	Crystal lattice parameters, Å	Lattice volume, Å <sup>3</sup>	Database card number PDF2	Phase content, %
CdSe	CdSe	Cubic	F-43m(216)	a=6.11050 ( <i>a<sub>etalon</sub></i> =6.0500)	228.16	PDF-03-065-2891	100

Macro stresses were estimated from the analysis of the diffraction peak displacement calculated according to the equation (2):

$$\text{macrostrain} = \frac{d_{exp} - d_{pristine}}{d_{pristine}}, \quad (2)$$

where  $d_{pristine}$  and  $d_{exp}$  - experimental and reference interplanar distances, respectively. Lattice stresses and macrostresses in the structure were estimated for the three most intense diffraction peaks with Miller indices (111), (220) and (311). Table 2 presents the data on changes in the macrostresses in the structure. The crystalline density was calculated using the formula (3):

$$\rho = \frac{1.6602 \sum AZ}{V_0}, \quad (3)$$

where  $V_0 = \frac{\sqrt{3}}{2}a^2c$  is the volume of the hexagonal cell,  $Z$  is the number of atoms in the crystal cell,  $A$  is the atomic weight of the atoms. The results are presented in table 2. The average crystallite size was calculated using the Scherer equation (4):

$$L = \frac{k\lambda}{\beta \cdot \cos(\theta)}, \quad (4)$$

where  $k = 0.9$  is the dimensionless coefficient of particle shape (Scherer constant),  $\lambda = 1.54 \text{ \AA}$  is the X-ray wavelength,  $\beta$  is the half-width of the half-height reflex (FWHM) and  $\theta$  is the diffraction angle (Bragg angle).

Table 2.

Data changes in element composition.

No.	Macrostresses			Density, g/cm <sup>3</sup>	Average crystallite size, nm
	(111)	(220)	(311)		
CdSe	0.012	0.009	0.010	5.569	3.74±0.23

## Results. Optical properties of QD

It is known that optical spectroscopy is one of the most widely-accepted analytical methods used to determine QD characteristics. The smallest energy absorption function (peak of exciton absorption) can give primary data on the size of the forbidden band  $E_g$ , particle size  $D$ , and other parameters [11]. Figure 2 shows normalized optical absorption spectra of unpurified CdSe QDs samples: 2a) – Series No.1, QD synthesis at 170 °C, 210 °C and 240 °C using a surface stabilizer like trioctylphosphine (TOP); 2b) – Series No. 2, QD-synthesis at 240 °C with a different ratio of stabilizers TOPO:HDA = 66:33; 50:50; 33:66 (in all cases the TOP number is the same); 2c) – Series No. 3, QD- synthesis of hexagonal and cubic structures at 240 °C.

In order not to overload the graphs with details, the optical absorption spectra are given only for QD-samples of series No. 1 obtained at 240 °C and QD- samples of CdSe cubic structure, series No. 3.

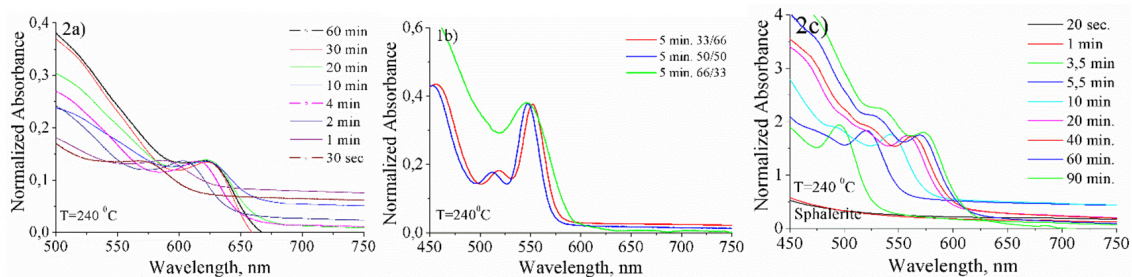


Figure 2. Optical absorption spectra of CdSe QDs for objects No.1, No.2, No.3.

It is seen from the optical absorption spectra that with an increase in the growth temperature, the peak of the exciton absorption monotonically shifts to the long wavelength region of the spectrum, demonstrating growth of nanoparticles. The study of the absorption spectra showed that the QD-dimensions of series No. 1 ( $T=240^{\circ}\text{C}$ ) grow from 3.17 nm to 5.75 nm, the growth rate is 0.04 nm/min; at  $T=210^{\circ}\text{C}$ , the QD-size grows from 2.44 nm to 5.70 nm, the growth rate is 0.032 nm/min; at  $T = 170^{\circ}\text{C}$ , QD- sizes grow from 2.10 nm to 3.95 nm with a growth rate of 0.03 nm/min, the results are shown in Figure 3a. The QD-diameters and growth rates for the samples of series No. 2 and No. 3 are determined, the graphs are shown in Figures 3b, 3c.

As can be seen from Figures 3a, 3b, 3c, it is the high synthesis temperature that determines the initial size of the nucleus of the nanocrystal and its growth rate. QD samples demonstrate a sharp increase in the linear dimensions of nanoparticles followed by a plateau, signaling about termination of the nanocrystal growth. The figures show the increase in the synthesis temperature causes faster consumption of the growth material. Comparison of graphs for QD-samples, series No. 1, No. 2 and No. 3, shows that the use of additional surface stabilizers like HDA: TOPO eliminates Ostwald's ripening allowing particles to grow pseudo-linearly minimizing the growth rate (compare Figures 3a, 3b and 3c).

Thus, to obtain large nanocrystals of 6 nm and more, additional injection of precursors is required. As for temporal characteristics of nuclei formation and nanocrystal growth, it was shown in earlier works by in-situ methods [14] that

for CdSe QDs (170 °C) formation of nuclei starts from the first minute with the formation of a nanocrystal to the second. Then nanocrystals start to grow. It is obvious that an increase in the synthesis temperature accelerates these processes.

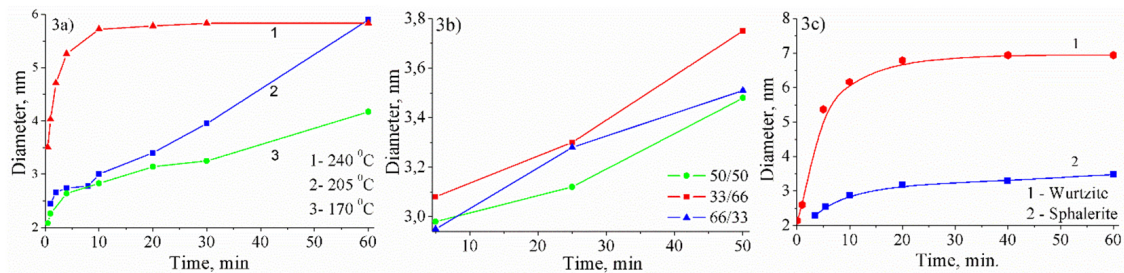


Figure 3. Dependence of diameter of CdSe quantum dots on time for the series of No. 1, No. 2, and No. 3.

## Investigation of luminescent properties

The QD luminescence was studied at room temperature under excitation by photons with a wavelength of 350 nm. The excitation of luminescence by photons 350 nm was determined from the excitation spectra of QDs. The QD excitation spectra are not shown in order not to clutter up the graphs; Also, the  $\lambda_{350\text{ nm}}$  was chosen due to the presence of a second luminescence band of the reference standard - rhodamine 6G. Figures 4a, 4b, 4c show the luminescence spectra of the QD samples.

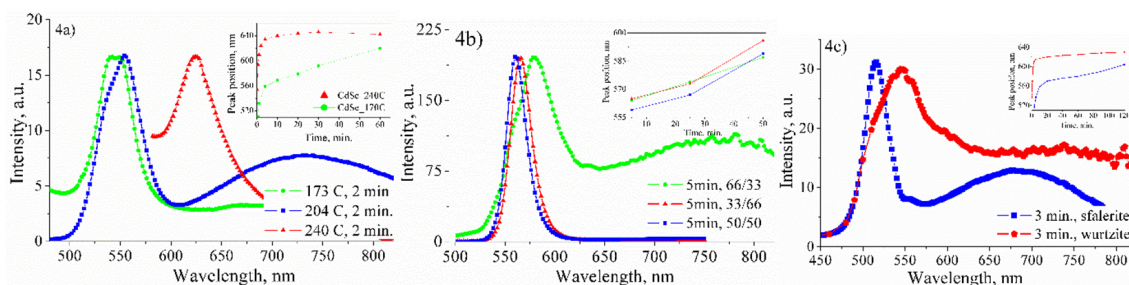


Figure 4. Luminescence spectra of the QD- samples of series No. 1-3.

It was noticed that an increase in the synthesis temperature leads to a shift of the luminescence band to the long-wave region of the spectrum. According to the results of spectra processing, the dependence of the position of the luminescence peak on the synthesis time was obtained (see the inserts in Figures 4b, 4c, not to overload the graphs in the figures, only part of the measured spectra is shown). It is seen from the figures that an increase in temperature and synthesis time leads to a shift of the luminescence peaks in the long-wave region, which is caused by the growth or increase in the size of nanocrystals. Then the curve goes to the plateau, and the growth slows down. However, addition of a mixture of surface stabilizers HDA:TOPO to the reaction mass provides the pseudo-linearity of the curve (see inset of Figure 4b). In Figures 4, in addition to the luminescence band at 556 nm, a band in the near infrared region of the spectrum is also visible. According to the authors [15], this band is due to the presence of selenium vacancies on the QD's

surface, i.e. is associated with superficial QD defects. This band disappears as the synthesis time increases.

The study of the luminescence spectra allows us to make some conclusions about polydispersity of the synthesized nanoparticles. For this purpose, the full width at half height (FWHM) of the band. FWHM of the luminescence peak is a measure of polydispersity and "purity" of the emission.

Investigation of this parameter is especially useful for obtaining luminescent materials, for example, for light-emitting technology with a "pure color" emission with a narrow distribution of sizes. Also, it is a good indicator of focusing or defocusing of nanoparticle sizes at continuing growth. It is mentioned in literature that the FWHM value lying within (30–40) nm indicates monodispersity of the synthesized nanoparticles [4]. For some QD samples, we determined the FWHM values. Figure 5 shows the average FWHM values obtained from the luminescence spectra of the QD samples.

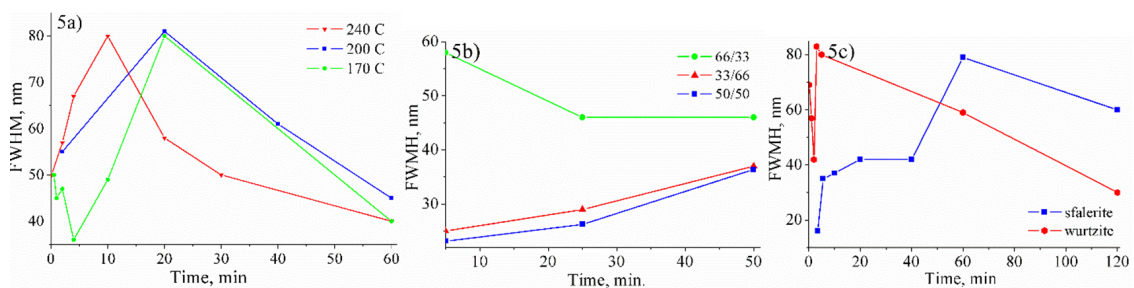


Figure 5. FWHM of QD spectra for series No. 1-3.

Figure 5a for samples of series No. 1 shows a sharp increase in the FWHM value at the initial 10th and 20th minutes, followed by a decrease. A similar behavior was also observed for QD samples of No. 3 series. A drop in FWHM with a continuing growth of nanoparticles means the establishment of a focusing mode, i.e. establishing of a narrow distribution in sizes of the synthesized nanoparticles. This is the mode in which the "ensemble" of nanoparticles tends to monodispersity. However, for samples of series No. 2, the opposite behavior is observed.

A similar behavior is observed for QY. After the initial increase, the QY value stabilizes at rather low values after the 10th minute for series No. 1, and after the 20th minute for the samples of series No. 3.

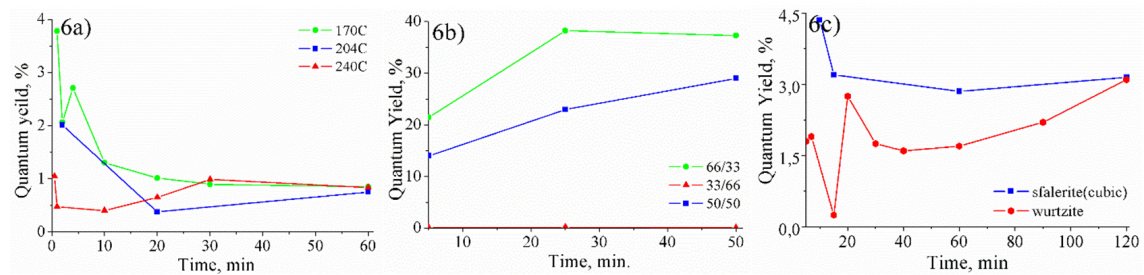


Figure 6. Quantum output of QD-luminescence for series No.1-3.

However, quite the opposite behavior is observed for FWHM and QY for samples of series No. 2. This behavior requires further detailed study. As can be seen from Figure 2b, the additional stabilizers increases QY, reaching a maximum

with a ratio of (66:33). Thus, the study of the luminescent properties of objects confirms that the use of a mixture of additional stabilizers like HDA: TOPO with the constant presence of TOP causes a sharp increase in the QY value.

Studies of the effect of surface stabilizers showed that the use of a separate mixture such as TOPO:TOP; HDA:TOP; HDA:TOPO:TOP; gives QY values of 5.3%, 10.1% and 13.1%, respectively

## Conclusion

In this work, the role of temperature and synthesis time, the influence of the coordinating solvent, its proportions on the polydispersity and the quantum yield of luminescence of nanoparticles are studied. Focusing and defocusing modes were determined. It was demonstrated that using a mixture of HDA: TOPO: TOP in a ratio of (66:33:1) allows us to obtain QDs with QY=39%. It was experimentally observed that an increase in the synthesis temperature accelerates the growth of particles and the size of the nucleus (see Figure 2).

## Acknowledgement

The authors express their gratitude to the Committee of Science MES RK for financial support in carrying out research, IRN AP05131725 "Luminescent converters of solar radiation based on quantum dots of semiconductors to increase the efficiency of existing silicon solar cells", IRN AP05132165 "Development of technology for producing asphaltenes from petroleum raw materials as organic semiconductors for nanoelectronics" for (2018–2020).

## References

- [1] Y. Cheng et al., *Nanophotonics* **5** (2016) 31-54.
- [2] G.H.Carey et al., *Chem. Rev.* **115** (2015) 12732-12763.
- [3] L. Qu, X. Peng, *J. AM. CHEM. SOC.* **124** (2002) 2049-2055.
- [4] C. de Mello Donega et al., *J. Phys. Chem. B* **107** (2003) 489-496.
- [5] I. Mekis et al., *J. Phys. Chem. B* **107** (2003) 7454-7462.
- [6] D.V. Talapin et al., *Nano letters* **1** (2001) 207-211.
- [7] D.V. Talapin et al., *J. Phys. Chem. B* **108** (2004) 18826-18831.
- [8] A.I. Ekimov, A.L. Efros, *Phys. Status Solidi B-Basic Res.* **150** (1988) 627-633.
- [9] E.S.Speranskaya, *Kvantovye tochki na osnove selenida kadmija: poluchenie, modifikacija i primenenie v immune himicheskomanalize (Avtoreferat dissertacii, Saratov state university, 2013) 23 p. (In Russian)*
- [10] J. Jasieniak et al., *J. Phys. Chem. B* **109** (2005) 20665-20668.
- [11] W.W. Yu et al., *Chem. Mater.* **15** (2003) 2854-2860.
- [12] S.N. Contreras Ortiz et al., *Journal of Physics: Conference Series* **687** (2016) 012097.
- [13] M. Grabolle et al., *Anal. Chem.* **81** (2009) 6285-6294.

- [14] T.N. Nurakhmetov et al., Proceeding of the IX International conference «Efficient use of resources and environmental protection – key issues of mining and metallurgical complex development» and XII International science conference «Advanced technologies, equipment and analytical systems for materials and nanomaterials», Oskemen **1** (2015) 315-323.
- [15] R.W. Meulenberg et al., Nano letters **4** (2004) 2277-2285.